

"In Vivo Characterization of Brain Ultrashort-T2 Components" Supporting Information

List of Figures

- S1 Water sphere phantom results demonstrating the importance of randomized TE ordering for accurate relaxometry at 7T (3T results shown in Fig. 3. The acquisition strategy is shown in Fig. 1. The sequential TE ordering has unexpected signal fluctuations, even at the same TE (red arrows), whereas the random TE ordered data better represents the expected mono-exponential decay. 2
- S2 Representative UTE images and parameter maps from a two-component fit at 3T and 7T. The ultrashort- and long- T_2^* component maps are only shown for regions with AIC values less than -260 (3T) and -235 (7T). The ultrashort- T_2^* components were calculated based on the fat-frequency reconstruction, whereas the long- T_2^* components were calculated based on the water-frequency reconstruction. 3
- S3 Whole-brain histograms of the T_2^* and frequency offset, corrected for B0 inhomogeneity, of the ultrashort- T_2^* component at 3T and 7T for all 5 volunteers using a two-compartment signal model. The dashed lines indicate the median values across the entire brain but excluding regions of poor fitting based on the AIC with the same criteria as in Fig. S2. 4

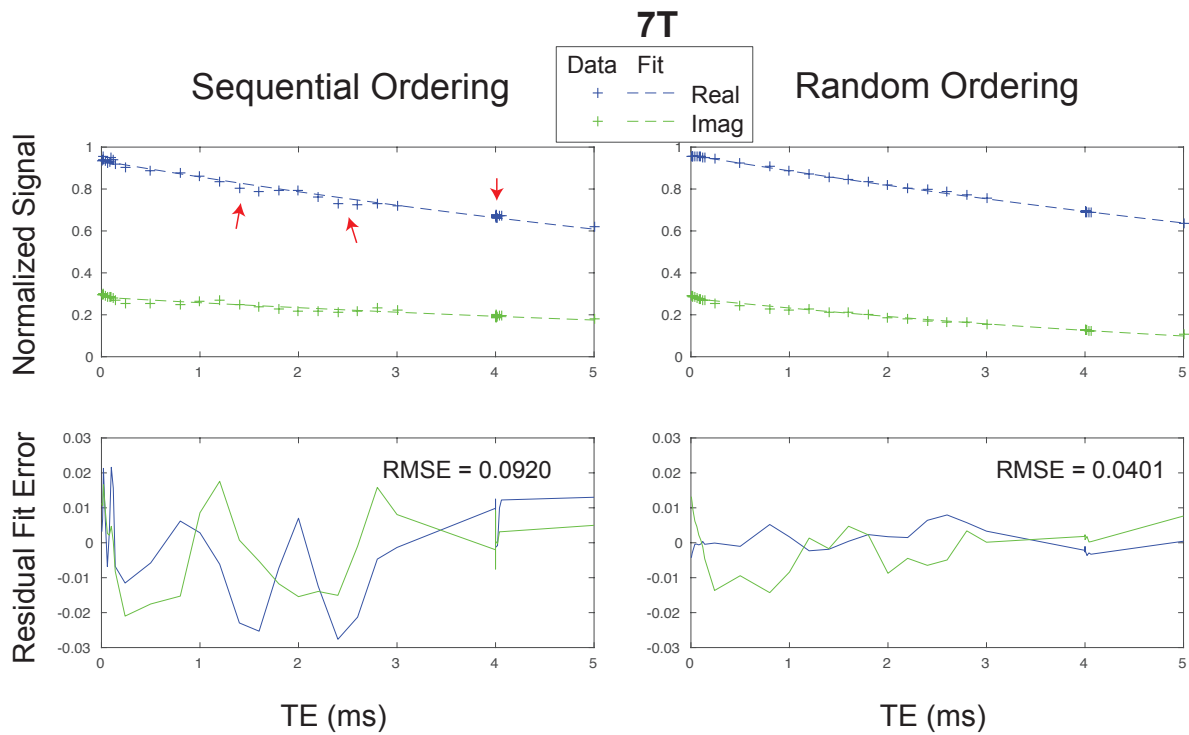


Figure S1: Water sphere phantom results demonstrating the importance of randomized TE ordering for accurate relaxometry at 7T (3T results shown in Fig. 3. The acquisition strategy is shown in Fig. 1. The sequential TE ordering has unexpected signal fluctuations, even at the same TE (red arrows), whereas the random TE ordered data better represents the expected mono-exponential decay.

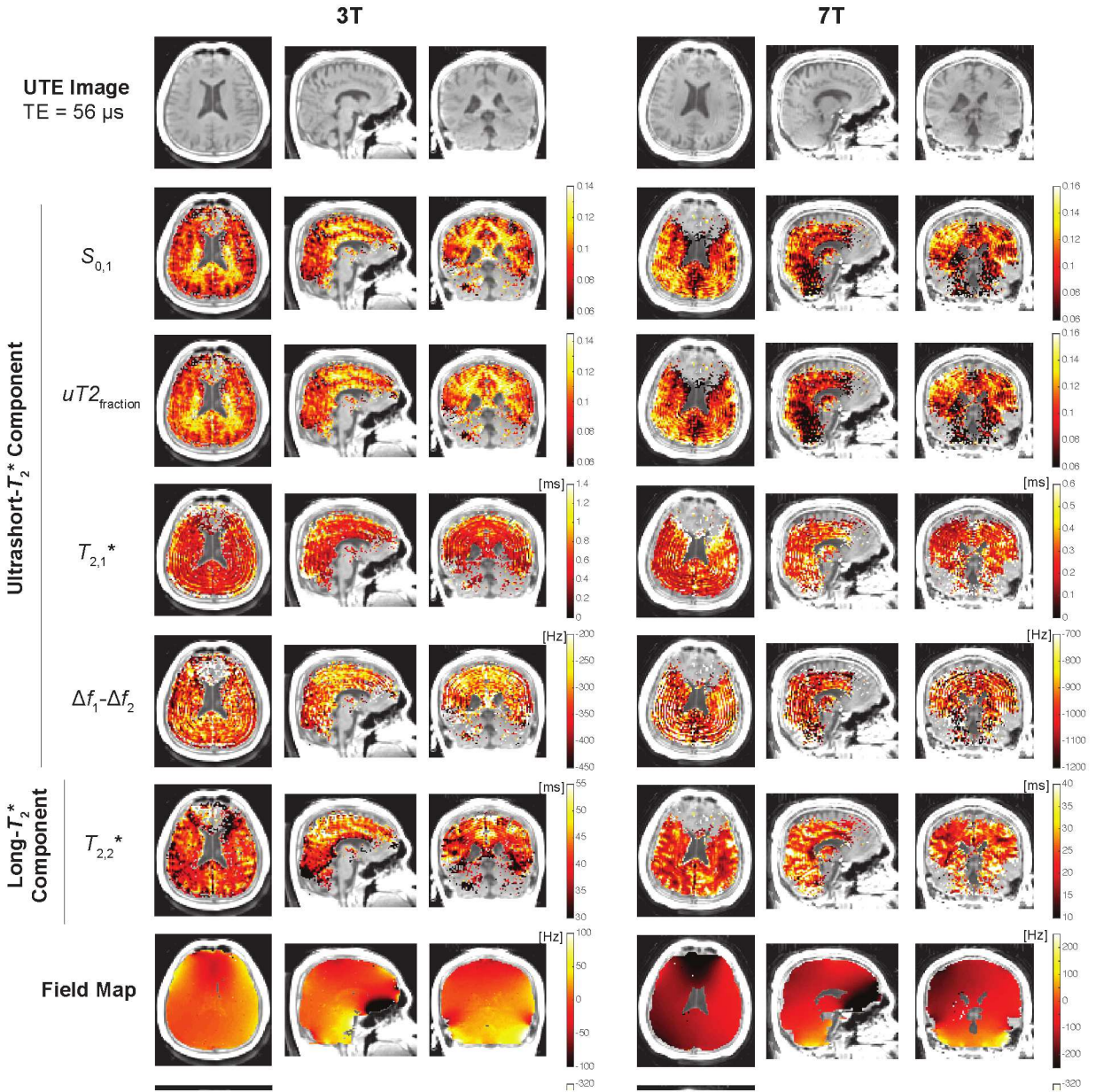


Figure S2: Representative UTE images and parameter maps from a two-component fit at 3T and 7T. The ultrashort- and long- T_2^* component maps are only shown for regions with AIC values less than -260 (3T) and -235 (7T). The ultrashort- T_2^* components were calculated based on the fat-frequency reconstruction, whereas the long- T_2^* components were calculated based on the water-frequency reconstruction.

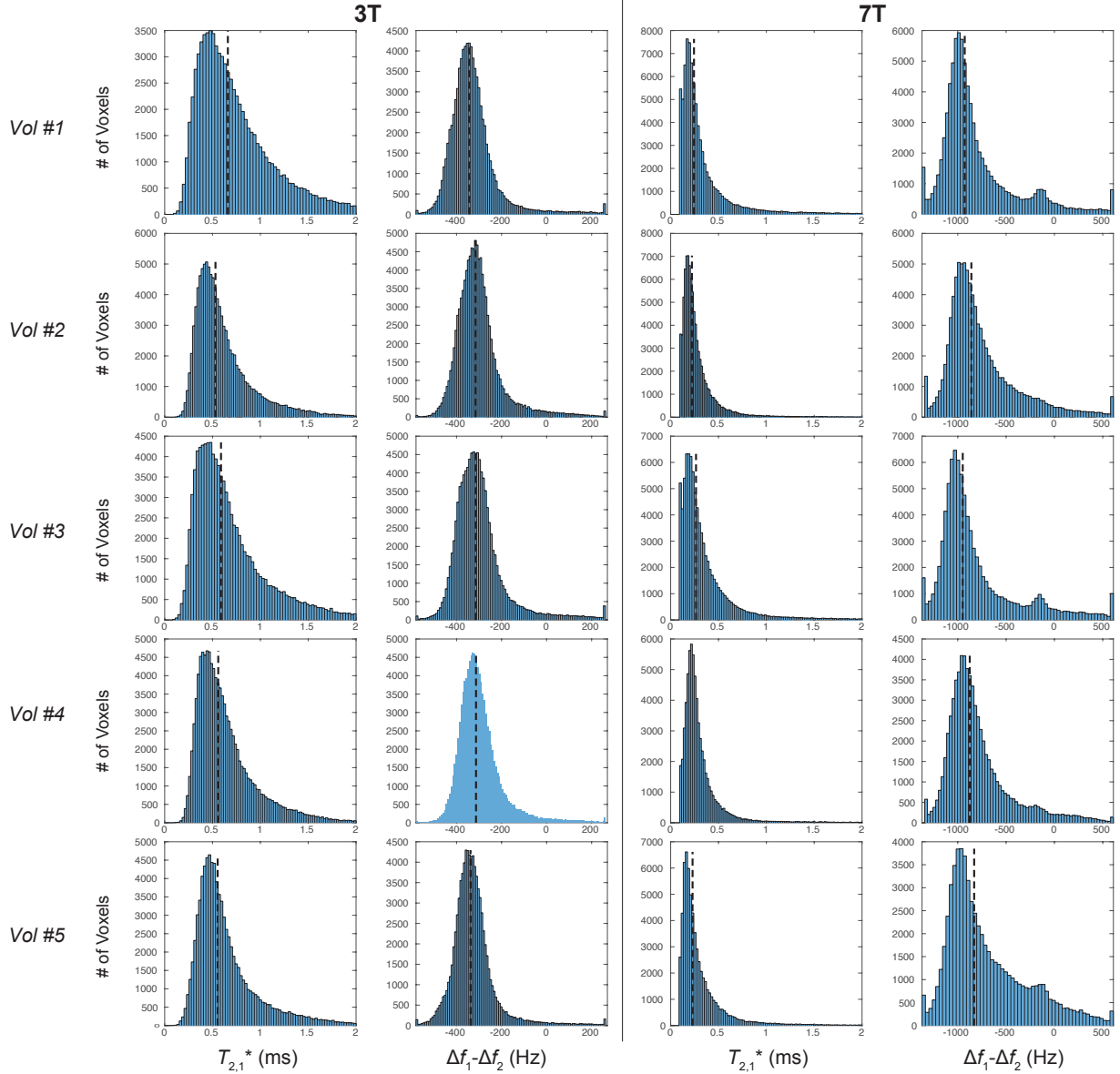


Figure S3: Whole-brain histograms of the T_2^* and frequency offset, corrected for B0 inhomogeneity, of the ultrashort- T_2^* component at 3T and 7T for all 5 volunteers using a two-compartment signal model. The dashed lines indicate the median values across the entire brain but excluding regions of poor fitting based on the AIC with the same criteria as in Fig. S2.